UNIVERSITY OF LEEDS

Article:
Tai, K, Rappolt, M orcid.org/0000-0001-9942-3035, Mao, L et al. (3 more authors) (2020) The stabilization and release performances of curcumin-loaded liposomes coated by high and low molecular weight chitosan. Food Hydrocolloids, 99. 105355. p. 105355. ISSN 0268-005X

https://doi.org/10.1016/j.foodhyd.2019.105355

The stabilization and release performances of curcumin-loaded liposomes coated by high and low molecular weight chitosan

Kedong Tai [a], Michael Rappolt [b], Like Mao [a], Yanxiang Gao [a], Xin Li [c], Fang Yuan [a,*]

[a] Beijing Advanced Innovation Center for Food Nutrition and Human Health, Beijing Laboratory for Food Quality and Safety, Beijing Key Laboratory of Functional Food from Plant Resources, College of Food Science & Nutritional Engineering, China Agricultural University, Beijing 100083, P.R. China

[b] School of Food Science and Nutrition, University of Leeds, Leeds LS2 9JT, U.K.

[c] School of Food Science, Jiangnan University, Wuxi, Jiangsu, 214122, P.R. China

*Corresponding author (Fang Yuan).

Tel: +86-10-62737034

Address: Box 112, No.17 Qinghua East Road, Haidian District, Beijing 100083, China

E-mail: yuanfang0220@cau.edu.cn

ABSTRACT

A comprehensive stability evaluation for curcumin-loaded liposomes (Cur-LP) coated by low (LCS) or high (HCS) molecular weight chitosan with three gradient concentrations (L: low; M: medium; H: high) was the main objective of this study. Apart from leading to a higher encapsulation efficiency (> 90%), all chitosan-coated Cur-LP displayed an improved stability with respect to resistant to salt, sunlight, heat, accelerated centrifugation and long-term storage at 4 °C. Increasing the molecular weight and concentration of chitosan could effectively improve the stability of Cur-LP, in which HCS-H coatings displayed the best performance. According to the fluorescence probe analysis, the mechanical reinforcement of liposomes and the concomitant reduction in membrane fluidity accounts for the major contribution to vesicle stability. Secondly, a simulated digestion model was used to prove the applicability of sustained curcumin release, achieved by adjusting the molecular weight and concentration of the chitosan stabilizer for Cur-LP. The results of this study show that high molecular weight chitosan used at relatively high concentrations, is a promising coating material for improving the stability and sustained release of Cur-LP *in vitro*.

KEYWORDS: liposomes; curcumin; chitosan; vesicle stability; sustained release

1. Introduction

In recent years, the bioactive properties of curcumin have been widely investigated, including antioxidant, anti-inflammatory, antimicrobial and anticarcinogenic activities (Anand, Kunnumakkara, Newman, & Aggarwal, 2007). Curcumin is a hydrophobic polyphenol extracted from the rhizome of herb *Curcuma longa*. Although it has been used as traditional Chinese medicine for centuries, three principle limitations were not addressed until modern medical studies have focussed on this bioactive compound: (ⅰ) low solubility, (ⅱ) easy degradability and (ⅲ) poor bioavailability (Nelson, et al., 2017). As a matter of fact, the hydrophobicity and rapid metabolism of curcumin are the main culprits, preventing people from to benefit from it. In fact, its bioavailability reaches only 1% after oral administration (Liu et al., 2016). Several delivery strategies have been employed to overcome these obstacles, such as designing emulsions (Ma, et al., 2017), micelles (Wang & Gao, 2018), hydrogels (Zheng, Zhang, Chen, Luo, & McClements, 2017) , nanoparticles (C. Tan, Xie, Zhang, Cai, & Xia, 2016), applying electrospun fibres (Alehosseini, Gomez-Mascaraque, Martinez-Sanz, & Lopez-Rubio, 2019), creating phospholipid complexes (Maiti, Mukherjee, Gantait, Saha, & Mukherjee, 2007) and using liposomal systems (Alavi, Haeri, & Dadashzadeh, 2017; Karewicz et al., 2013; Liu, Liu, Zhu, Gan, & Le, 2015; Pu, Tang, Li, Li, & Sun, 2019). From nutrition and safety perspectives, liposome are recognized having great potential as nutraceutical carriers. They form by self-assembly of commonly used phospholipid molecules, and display an onion-like architecture consisting of altering lipid and water

layers with a central water core. These liposomes are also known as multi-lamellar vesicles (MLVs), or when only bilayer is given, as unilamellar vesicles (ULVs). In spite of biocompatibility, biodegradability, nontoxicity, and non-immunogenicity as advantages for liposomes (Li et al., 2019), their bad physicochemical stability severely limits the application in the food industry as well as in pharmacy. One reason for poor stability lies in the high sensitivity to chemical degradation of phospholipids by hydrolysis of the ester groups and oxidation of unsaturated acyl chains, which facilitate the structural disruption of liposomal membranes. Another reason for poor stability is caused by vesicle fusion, which induces larger vesicles and sedimentation. Finally, the phase separation of hydrophobic bioactive compounds from lipid bilayer can occur due to lipid degradation and/or temperature fluctuations, which also leads to the leakage of the embedded bioactive compounds (Grit & Crommelin, 1993). Thus, how to decrease the susceptibility to environmental stress and achieve an efficient utilization liposomes is still attracting growing interest.

Compared with tedious protocols for modifying the composition of liposomal membranes, surface coating has been identified as economical and effective method to improve stability (He et al., 2019). Among numerous coating materials, chitosan is a well-considered choice to form protective polyelectrolyte layers due to the positive charges that readily interact with negatively charged liposomal surfaces. In addition, the biocompatible and biodegradable polysaccharides have been permitted to be used in food products, such as for antimicrobial and preservative films applied in food

storage (Mujtaba et al., 2019). The chitosan-coating method has been proposed many years ago (Henriksen, Smistad, & Karlsen, 1994; Henriksen, Vagen, Sande, Smistad, & Karlsen, 1997) and has been applied in several bioactive compounds-loaded liposomes in recent years, concerning the up-take of resveratrol (Park, Jo, & Jeon, 2014), quercetin (Hao et al., 2017), peptides (Gradauer et al., 2013), and curcumin (Karewicz et al., 2013; Li et al., 2017; Liu et al., 2015). Nevertheless, we note that nearly all studies have focused on only one type of chitosan or on its modified derivative. Apart from its stabilization properties, Cuomo et al. found that chitosan coating could also significantly improve the absorption of curcumin in liposomes, shown by *in vitro* digestion analysis (Cuomo et al., 2018). This is mainly attributed to the improvement of mucoadhesive properties of chitosan-coated vesicles (Shin, Chung, Kim, Joung, & Park, 2013). Further, study focusing on the thermal stability comparison between chitosan-coated and uncoated Cur-LP, demonstrated that chitosan coatings effectively protect curcumin from degradation and drastically reduce leakage (Liu et al., 2015). As to chitosan derivatives, Tian et al. studied the potential of carboxymethyl and quaternary ammonium chitosan-coated liposomes and found that the chitosan derivatives-coated liposomes displayed a six folds higher bioavailability of curcumin after oral administration, when compared to uncoated ones (Tian et al., 2018). Thiolated chitosan was also synthesized to be applied in Cur-LP, which led to a slower *in vitro* release and a higher stability above room temperature (Li et al., 2017). Apart from single-layered chitosan coatings utilized in the above studies, multi-layered chitosan

104 coatings were also formed to evaluate the protective efficacy for liposomes (Jeon, Yoo,
105 & Park, 2015). Layer-by-layer coatings were prepared by electrostatic deposition of
106 positively charged chitosan and other negatively charged polyelectrolytes. Also these
107 stabilised liposomes exhibited an improved sustained release property for embedded
108 bioactive compounds.

109 With respect to the different molecular properties of chitosan on liposomes,
110 previous studies have revealed that increasing the molecular weight and concentration
111 improved physical stability of liposomes to some extent (Filipovic-Grcic, Skalko-
112 Basnet, & Jalsenjak, 2001; Laye, McClements, & Weiss, 2008), as well as improved
113 the hypoglycaemic efficacy after oral administration in mice (Wu, Ping, Wei, & Lai,
114 2004). For chitosan derivatives, molecular modifications were tested for possible usage
115 in liposomes, while the oral safety of materials needs further biological evaluation. This
116 concerns in particular the recommended administered dosage, because the toxicity of
117 chitosan increases with increasing charge density of the molecule (Kean & Thanou,
118 2010). In view of curcumin-loaded liposomes, although several studies have illustrated
119 the feasibility and improved stability throughout chitosan coating, only low or medium
120 molecular weight chitosan or derivatives have been so far investigated (Cuomo et al.,
121 2018; Karewicz et al., 2013; Liu et al., 2015).

122 To address this issue, we undertook an evaluation study on low and high molecular
123 weight chitosan used in the preparation of Cur-LP by the thin film hydration method.
124 Additionally, low, medium and high concentrations of each chitosan were investigated.

A library of Cur-LP coated with chitosan was prepared for stability and *in vitro* release performance comparisons, such as environmental stress (salt, light, and heat) and long-term storage. We illustrate how molecular weight and different concentrations modulate the stability and release profile of Cur-LP, with promising results for the development of chitosan-coated liposomes for potential applications in healthcare products and drug therapy in the future.

2. Materials and methods

2.1 Materials and chemicals

Soybean lecithin (Lecigran 1000P, powdered soybean lecithin containing a mixture of phospholipids, such as phosphatidylcholine, phosphatidylethanolamine and phosphatidylserine; acetone insoluble substance content > 96%) was obtained from Cargill Asia Pacific Food System Co., Ltd (Beijing, China). Curcumin (> 95% purity) was obtained from Hebei Food Additive Co., Ltd (Hebei, China). Cholesterol was purchased from the Sinopharm Chemical Reagent Co., Ltd (Shanghai, China). Chitosan with low molecular weight (MW=50-190 kDa, deacetylation degree > 75%) and high molecular weight (MW=310-375 kDa, deacetylation degree > 75%), pyrene (≥ 99%), 1,6-Diphenyl-1,3,5-hexatriene (DPH, 98%), mucin from porcine stomach (M2378), pepsin from porcine gastric mucosa (P7125, enzymatic activity ≥ 400 units/mg protein), pancreatin from porcine pancreas (P1750, 4 × USP) and bile salts were purchased from Merck (Shanghai, China). Triton X-100 was purchased from Xi Long Chemical Co.,

Ltd (Guangzhou, China). All other reagents used were analytical grade without further purification.

2.2 Preparation of Cur-LP coated with chitosan

Cur-LP was prepared by the thin film hydration method combined with high-pressure homogenization, which reduces the vesicle size and improves the liposomal homogeneity. The chloroform solvent containing soybean lecithin, cholesterol, and curcumin (5:1:0.125, w/w/w) was vacuum-desiccated on a rotary evaporator to form a thin lipid film over the inside surface of a round-bottom flask. This procedure lasted for at least 30 min in order to remove residual chloroform. Then, the lipid film was hydrated with acetate buffer (0.05M, pH 5.0) and subjected to weak sonication for eluting the film easier. The obtained coarse liposome suspension was homogenized using high-pressure homogenization (80 MPa, three cycles) for decreasing the vesicle sizes of Cur-LPs. The fortified concentration of soybean lecithin was 10 mg/mL.

The prepared Cur-LP dispersion was added dropwise into LCS and HCS solution (dissolved in the same acetate buffer described above) by peristaltic pump at the volume ratio of 3:5 combined with magnetic stirring for 60 min. The dropping speed was 2.5 mL/min. Based on the pre-set gradient concentrations of each chitosan (1, 2.5 and 5 mg/mL, respectively), final concentrations of chitosan were diluted to 0.625, 1.563 and 3.125 mg/mL after mixing with Cur-LP dispersion. These three concentrations are referred to as low (L), medium (M) and high (H) concentration of chitosan. Accordingly, LCS-L (-M, -H) and HCS-L (-M, -H) define Cur-LP coated by low and high molecular

weight chitosan with low (medium, high) concentrations. Respectively. Chitosan-coated Cur-LP was stored in refrigerator at 4 °C for further analysis.

2.3 The vesicle characterization of liposomes

The vesicle size, zeta potential, and size distribution were determined by dynamic light scattering (DLS) using Malvern ZetasizerNano-ZS90 (Malvern Instruments Ltd., UK). Samples were 10-fold diluted with acetate buffer for fear of the multiple scattering that influences the data accuracy. Each sample was equilibrated in the instrument for 2 min before test.

The encapsulation efficiency (EE) of curcumin in liposomes was determined by absorbance using UV-1800 spectrophotometer (Shimadzu, Japan). Firstly, liposomes were centrifuged (15000 × *g*) to remove the probably absorbed or dissociated curcumin on the vesicle surfaces or medium. The sedimentation was re-dispersed by buffer and centrifuged again. This procedure was repeated for three times to remove the unembedded curcumin as much as possible. Finally, the sedimentations were disrupted by Triton X-100 and methanol, and the originally encapsulated curcumin dissolved in methanol was detected by its absorbance band at 428 nm. Primary Cur-LP was treated in the same way as sedimentation described above for determining the gross amount of curcumin. The EE of curcumin was calculated using the following equation:

$$\mathrm{EE}(\%) = \frac{\text{Amount of encapsulated curcumin}}{\text{Total amount of curcumin}} \times 100 \quad (1)$$

2.4 TEM

The microstructures of liposomes were observed by JEM-1200EX transmission electron microscope (TEM, Japanese Electronics Co., Ltd, Japan). The freshly prepared liposomes, which were diluted beforehand, were transferred on a 200-mesh carbon-coated copper grid. Then, samples were negatively stained by uranyl acetate solution (3%) for 90 s and air-dried at room temperature. Excessive liquid could be removed using filter paper if necessary. TEM images of liposomal vesicles were captured at an accelerating voltage of 100 kV.

2.5 Stability studies

2.5.1 Salt stability

The stability of liposomes against salts stress was evaluated by incubating them in NaCl solutions with different concentrations (100-1000 mM) at room temperature for 1 h. The relative change rate of vesicle size (ΔS) and net zeta potential (ΔP) were calculated using the following equation:

$$\Delta S(\Delta P) = \frac{\text{Vesicle size (|zeta potential|) after incubation}}{\text{Vesicle size (|zeta potential|) in initial}} \times 100 \quad (2)$$

2.5.2 Photo stability

All liposomes were transferred into transparent glass tubes and sealed by rubber stoppers. The simulated solar irradiation was performed using a xenon test chamber (Q-SUN, Xe-1-B, Q-Lab Corporation, Ohio, USA) for 6 h. At predetermined irradiation time, an aliquot of treated sample was adequately dissolved into anhydrous methanol followed by centrifugation. The supernatant was collected to determine the concentration of residual curcumin in samples by absorbance. The curcumin retention

rates (%) after different periods of irradiation were calculated using the following equation:

$$\text{Curcumin Retention (\%)} = C_t / C_0 \times 100 \quad (3)$$

Where C_0 and C_t are concentrations of curcumin in initial and in different sampling time, respectively.

2.5.3 Thermal stability

The thermal stability of Cur-LP was evaluated at 80 °C in a water bath combining light avoidance. Similar to the operation in photo stability evaluation, samples taken at pre-set time intervals were also mixed with anhydrous methanol. After centrifugation, the absorbance of collected supernatant was measured by UV-vis spectrophotometry at 428 nm. The retention rates (%) of curcumin after different periods of heat treatment were calculated using the equation in photo stability evaluation.

2.5.4 Centrifugal stability

The centrifugal stability of liposomes was evaluated by a multi-sample analytical centrifuge LUMiSizer® (L.U.M GmbH, Berlin, Germany), which determines the physical stability by detecting the dynamic change of transmission intensity of dispersions in test tubes in terms of time and position. The evolution of transmission profile shows a continuously changing instability process during centrifugation, such as the vesicle migration and sedimentation. In this study, all liposomes were subjected to centrifugation at speed of 2000 rpm for 1 h. A total of 360 profiles were recorded in intervals of 10 s. Furthermore, the instability index was recorded by the SEPView®

229 software (L.U.M, Berlin, Germany), which can intuitively compare the differences of
230 instability between samples during centrifugation.

231 *2.5.5 Storage stability*

232 All curcumin-loaded liposomes were transferred into the sealed brown glass bottles
233 and stored at 4 °C for three weeks. The vesicle sizes and residual amounts of curcumin
234 in samples were monitored at scheduled time intervals during storage, the latter was
235 calculated using the same method and equation in section 2.5.2.

236 *2.6 The determination of membrane properties*

237 *2.6.1 Micropolarity in membranes*

238 Pyrene has high sensitivity to the environmental polarity which can be used to
239 manifest the order degree of molecular arrangement in membranes. Briefly, the pyrene
240 solution (2 mM in acetone) was mixed with liposomes (10-fold diluted) at a volume
241 ratio of 1:50. The mixture was vortexed and incubated overnight at 4 °C. The
242 fluorescence emission spectra ranging from 350 to 450 nm was collected using F-7000
243 fluorescence spectrophotometer (Hitachi High-Technologies, Tokyo, Japan) at the
244 excitation wavelength of 338 nm. The fluorescence intensity ratio (I_1/I_3) of first and
245 third pyrene monomer vibronic peak was calculated. A higher ratio value means higher
246 polarity.

247 *2.6.2 Fluidity of membranes*

248 As a rod-shaped fluorescence probe, DPH inserted into liposomal membranes was
249 tightly immobilized by adjacent phospholipid molecules. Hence, the inclination degree

of DPH caused by the undulation of membranes can be used to manifest the fluidity degree. This is called 'polarization (P)', which is independent of pyrene concentration. The DPH solution (2 μM in dimethyl sulfoxide) and liposome (10-fold diluted) were mixed at the volume ratio of 1:5. The mixture was incubated at room temperature for 60 min. The wavelength of excitation and emission were 360 nm and 430 nm, respectively. The emission intensities were collected from directions perpendicular and parallel to the exciting light. The polarization of DPH was calculated using the following equations:

$$P = (I_{0,0} - G \times I_{0,90})/(I_{0,0} - G \times I_{0,90}) \quad (4)$$

$$\text{With } G = I_{90,0}/I_{90,90} \quad (5)$$

where $I_{0,0}$, $I_{0,90}$, $I_{90,0}$, $I_{90,90}$ are fluorescence intensities of emitted light (exciting light) polarized to exciting light (emitted light) in parallel (0) and vertical (90), respectively. G is the grating correction coefficient. The fluorescence intensity of DPH in the aqueous phase is almost non-detectable.

2.7 The release assay in vitro simulated digestion

2.7.1 The protocol of in vitro simulated digestion

In vitro simulated gastrointestinal tract (GIT) model was established to reveal the effects of molecular weight and concentration of chitosan on the release characteristics of curcumin in chitosan-coated liposomes. It included mouth phase (simulated saliva fluid, SSF, pH=6.8), gastric phase (simulated gastric fluid, SGF, pH=1.5) and small intestine phase (simulated intestinal fluid, SIF, pH=7.0) according to our previous study

(Tai et al., 2019). The whole simulated digestion process was carried out in a water bath shaking at 37 °C. All simulated digestive juices and liposomes should be preheated at 37 °C before mixing together. The detailed *in vitro* simulated digestion operation as follows:

Simulated mouth digestion was mixing liposomes with SSF (1:1, v/v) and took for 10 min. SSF was prepared by dissolving NaCl (1.594 g), KCl (0.202 g), and mucin (0.6 g) into 1 L of distilled water.

Simulated gastric digestion was mixing oral digestion with SGF (1:1, v/v) and took for 2 h. SGF was prepared by dissolving NaCl (2 g), concentrated HCl (7 mL), and pepsin (3.2 mg/mL) into 1 L of distilled water.

Simulated small intestine digestion was mixing stomach digestion with SIF (1:1, v/v) and took for 2 h. SIF was prepared by dissolving K_2HPO_4 (6.8 g), NaCl (8.775 g), bile salts (5 g), and pancreatin (3.2 mg/mL) into 1 L of distilled water. It was noteworthy that the pH of stomach digestion must be adjusted to 6.8-7.0 before mixing with SIF.

2.7.2 The determination of release profiles

The release property of curcumin from chitosan-coated liposomes was investigated by monitoring its release rate at predetermined time intervals during simulated digestion. 500 μL of digestive mixture was withdrawn from each phase and cooled down under an ice bath. For quantitative analysis of curcumin, the digestive mixture was centrifuged at 15000 × *g* for 30 min at 4 °C. The supernatant was collected to analyse the released amount of curcumin by absorbance. Note that, the release

amount of curcumin should be calculated by subtracting the free curcumin in initial without simulated digestion. The cumulative release rate (%) of curcumin was plotted as a function of time as follows:

$$\text{Cumulative release}(\%) = \sum_0^t \left(\frac{M_t}{M_0}\right) \times 100 \quad (6)$$

where M_0 and M_t are the initial amount of curcumin in liposomes without digestive treatment and the cumulative amount of released curcumin for each sampling in digestive medium, respectively.

2.8 Statistical analysis

All experiments were carried out in triplicate and data were expressed as mean ± standard deviation. One-way ANOVA and Duncan's significant difference test at 5% level of significance by IBM SPSS software version 25 (IBM Corp., NY) were performed. Data were processed using Origin 9.0 (OriginLab Inc., Northampton, MA, USA).

3. Results and discussion

3.1 Characteristics of chitosan-coated Cur-LP

The vesicle characteristics and encapsulation efficiencies of different chitosan-coated Cur-LP are summarized in Table 1, size distributions and TEM images are shown in Fig. 1. Compared with uncoated Cur-LP, the chitosan coating obviously increased the mean vesicle size of liposomes, but polydispersity index (PDI) result displayed opposite trends. The negatively charged Cur-LP (-45 mV) was changed to be

313 positive, when chitosan coating was introduced. It powerfully demonstrated the
314 successful coating of chitosan onto liposomal vesicles by electrostatic interaction
315 between the positively charged amine (NH_3^+) groups of chitosan and negatively
316 charged polar head groups of phospholipids (Henriksen et al., 1994; Zhou et al., 2018).
317 Because of no significant differences of zeta potential among different chitosan-coated
318 Cur-LP, the surfaces of liposomes can be thought of as completely covered by chitosan
319 in this study. As for concentration of chitosan, the vesicle size of Cur-LP increased with
320 the increase of chitosan concentration except for LCS-H. Generally, the results suggest
321 that higher chitosan concentration induce larger self-assembled aggregates on the
322 liposomal surfaces, which in turn lead to a thicker coating layer (Park et al., 2014). This
323 trend is also seen for HCS coatings, inducing even larger molecular aggregates that
324 leads to overall larger vesicle sizes. The exceptionally smaller size of LCS-H coated
325 liposomes can be attributed to the stronger hydrophobic character of LCS at higher
326 concentration (Tan et al., 2013). In this case, high concentrations cause chitosan to self-
327 aggregate in the buffer, leading to a partial dissociation phenomenon of the chitosan
328 layer. We note, that the different molecular weight and viscous property for HCS
329 eradicates this dissociation effect at higher concentrations (Pavinatto, Caseli, &
330 Oliveira, 2010). Laye et al. have investigated the relationship between chitosan
331 (medium molecular weight) concentration and vesicle size in bare liposomes. They
332 found that the vesicle size of chitosan-coated liposomes increased gradually, when the
333 chitosan concentration was greater than 0.5 mg/mL. The vesicle size was about 1000

nm when the concentration was 2 mg/mL (Laye et al., 2008), which is consistent with our results.

Although liposomes already had a satisfactory encapsulation capacity for curcumin with EE reaching up to 82% in this study, which is similar with result of a previous study (about 80%) (Choudhary, Shivakumar, & Ojha, 2019), the chitosan coating led to a clearly increased EE ranging from 95 to 99% (Table 1). We note, that for the different chitosan coatings with low and high molecular weight, no particular concentration dependence was observed (2% and 3% variation in EE for low and high molecular chitosan coatings, respectively; Table 1), and only slightly higher EE values were determined for HCS-coated liposomes compared with LCS-coated ones. Similar results were obtained in a study of resveratrol-loaded liposomes coating by chitosan (Park et al., 2014). Different results were obtained by Tan showing that chitosan coating slightly increased the EE of carotenoid in dependence of chitosan concentration (Tan, Feng, Zhang, Xia, & Xia, 2016). Slight reduction or disparities in EE with varying chitosan concentration might be attributable to liposomes coalescence during the centrifugation step (Li, Paulson, & Gill, 2015).

As shown in Fig.1, all Cur-LP display spherical shapes and coating layers are clearly observed in the formation of core-shell structures. Moreover, vesicles of all chitosan-coated Cur-LP dispersed well, apart from LCS-L sample, in which some bridging among vesicles appeared. Increasing chitosan concentration led to monodisperse suspension at the highest chitosan concentration.

3.2 The stability studies

3.2.1 Salt stability

Salt is commonly used as dietary sodium supplement in food product. Thus, it is essential to evaluate stability of liposomes subjected to salt solution with a gradient concentrations, which is shown in Fig. 2. The relative change rate of liposomal vesicle size was calculated for comparison. When NaCl concentration was below 200 mM, the decreased vesicle size were observed for all liposomes. This is mainly attributed to a decrease of electrostatic interaction between chitosan and liposomes caused by electrostatic screening effect of NaCl, and consequently, partial dissociation of chitosan from the surfaces of liposomes appeared (Liu et al., 2016). The corresponding zeta potential changes are shown in Fig. S1. However, as NaCl concentration is further increased, the vesicle size increases for Cur-LP, LCS-L and LCS-M. In particular, the LCS-L coated vesicles increases in size more than twice compared to Cur-LP at 600-1000 mM. A similar phenomenon was also obtained by the group of Cheng (Cheng et al., 2017). The vesicle size of Cur-LP prepared by the same method exhibited first a decrease followed by an increase in size as NaCl concentration further increased. Our study further found that both LCS and HCS at high concentrations improve the salt stability of Cur-LP. Note, that also the vesicle size variation as a function of salt concentration decreases. Concluding, larger molecular weight and higher concentration of chitosan render Cur-LP less sensitive to changes in salt concentration.

3.2.2 Photo stability

Due to the photosensitivity of curcumin, solar radiation is an important factor to consider, especially when it comes to long-term storage and shelf-life. In our previous study, the incorporation of β-sitosterol in Cur-LP improved the photo stability to some extent, when compared to liposomes without sterol (Tai, et al., 2019). In this study, the protective effect of chitosan on light degradation of encapsulated curcumin in liposomes was evaluated in terms of molecular weight and concentration. As shown in Fig. 3, the retention rate of curcumin in Cur-LP was much lower than chitosan-coated ones, which demonstrates that the protection of chitosan-covered vesicles works well for curcumin. We attribute the firm barrier formed by chitosan to improve the encapsulation properties of liposomes, and hence, make it harder to irradiate curcumin. Similarly, polyethylene glycol (PEG) coated on liposomes were also proved to effectively reduce light degradation of encapsulated doxorubicin (Bandak, Ramu, Barenholz, & Gabizon, 1999). Further, chitosan with different molecular weights have different protective effects on photo stability of Cur-LP. HCS protected curcumin from light degradation better than LCS as reflected in the higher retention rate of curcumin (Fig. 3). For the significantly different curcumin retention performance between LCS and HCS, we speculate that LCS does not form a uniformly-coated layer, whereas protective HCS layers are expected to display a better surface coverage (Desai, Liu, & Park, 2006). We note, that some aggregations were observed in TEM image for LCS-L, which worsened the leakage of curcumin. In conclusion, the thicker chitosan coating formed by HCS in combination with increasing concentrations reduces Cur-leakage. A

similar result was obtained by Li showing that HCS coatings performed better at protecting curcumin in emulsion (Li, Hwang, Chen, & Park, 2016). With respect to energy absorption by sunlight irradiation, also the thermal stability of chitosan-coated liposomes was investigated to further verify the barrier effect of chitosan coatings.

3.2.3 Thermal stability

It is obvious that thermal sensitivity for curcumin and high temperature applied in food products manufacturing like sterilization are irreconcilable. Therefore, an enhanced thermal stability is favourable to practical curcumin products. It has been proven that chitosan coating markedly protected curcumin from thermal degradation in liposomes (Liu et al., 2015). Concerning our work, the thermal stability of Cur-LP coated by LCS and HCS with different concentrations is shown in Fig. 4. Compared with the rapid decrease of curcumin retention rate for Cur-LP, where less than 60% of curcumin remained after 60 min, all chitosan-coated Cur-LP displayed better thermal stability, in which curcumin retention rates were over 80% after 60 min. Moreover, chitosan with higher molecular weight and concentration improved the thermal stability of Cur-LP. Particularly, more than 95% of curcumin was preserved in HCS-M or HCS-H coated liposomes after heat treatment. As previously reported, when liposomes go through the main phase transition, the coexistence of gel and fluid-crystalline phases lead to an increased membrane permeability, which induces the leaking out of curcumin (Hayashi, Kono, & Takagishi, 1998). The previous thermal and irradiation stability study emphasizes though that the barrier formed by chitosan coating conserves the

418 integrity of liposomal structure effectively and also maintains the stability of embedded
419 curcumin (Tan, Feng, et al., 2016). Here, the relatively strong electrostatic interaction
420 and steric hindrance effect provided by chitosan layers make major contributions to
421 stability. A similar protective effect was reported for chitosan-coated carotenoids-
422 loaded liposomes (Tan, Feng, et al., 2016). However, protection effects in this study
423 reached its saturation already at medium level concentrations, especially for HCS
424 coatings on liposomal surfaces and led no significant improvement in protection effects.

425 *3.2.4 Storage stability*

426 All prepared Cur-LP were kept in the refrigerator for monitoring the change rate of
427 vesicle size during three weeks storage, which is shown in Fig. 5. In the absence of
428 chitosan coating, vesicle size of Cur-LP increased dramatically in the first four days
429 and remained steady after that. On the contrary, LCS-L displayed a strong decrease in
430 vesicle size at the same time. Smaller vesicle size decrease were observed for LCS-M
431 and LCS-H coatings. This trend is mainly attributed to the partial dissociation of
432 chitosan from liposomal surfaces (Han, Shin, & Ha, 2012). In contrast, high
433 concentrations of chitosan suppressed this phenomenon and the smallest size variations
434 appeared in HCS-H coated liposomes. The initial increase of HCS-coated vesicle shows
435 that a firmer coating structure was formed in the beginning, even if the same size
436 decrease trend was observed afterwards. Two principle explanations can be contributed
437 to the initial size increase: one is the aggregation of small liposomal vesicles to form
438 uniform large aggregates (Li et al., 2015); another is seen in the continuous adsorption

439 of chitosan on surfaces of liposomes (Tan & Misran, 2012). Finally, the vesicle size of
440 HCS-L, HCS-M and HCS-H liposomes started to decrease on the 2nd, 7th and 14th
441 day, respectively. This further proves that chitosan with higher concentrations is
442 delaying the dissociation of coating from liposomes, which is in favour of size stability
443 of Cur-LP in storage.

444 *3.2.5 Centrifugal stability*

445 The last stability test concerned centrifugal stability of vesicles. Therefore, an
446 accelerated stability test was carried using a LUMiSizer centrifuge (Fig. 6). All
447 specimens were subjected to the same centrifugation force in the same period of time,
448 which facilitated the formation of liposomal sedimentation. As shown in Fig. 6, colours
449 of LUMiSizer transmission profiles change from red to green gradually representing
450 the dynamic changes in scanning time. The transmission rate on the top of sample cell
451 (nearby 110 nm) increased with the test time, which manifests continuous vesicle
452 migration towards the bottom of test cell. The overall increase of transmission rate
453 obtained in Cur-LP was regarded as rapid migration of vesicles to precipitation under
454 centrifugation. In contrast, clearly lower increases of transmission rate were observed
455 in chitosan-coated Cur-LP. The diverse transmission rate changes between upper and
456 lower parts of test cell, demonstrates a delay of vesicle migration. This phenomenon
457 was more significant when chitosan concentration was increased, no matter if LCS or
458 HCS. In other words, chitosan coating as well as increasing concentration effectively
459 improved physical stability of Cur-LP. Tan had also found a stability improvement of

carotenoid-loaded liposomes in the case of chitosan coating using the same detection method (Tan, Feng, et al., 2016). In order to quantize the difference of stability, instability index curves were determined (Fig. 6B). When a low chitosan concentration was used, LCS-L vesicles were more stable than HCS-L ones. As displayed in smaller curve slopes, smaller-sized vesicles move slower than bigger ones. When the chitosan concentration increased to medium level, similar slope indicated almost the same centrifugal stability between LCS-M and HCS-M liposomes. Above all, HCS-H vesicles had the best physical stability seen in the flat transmission profile as also described previously (Caddeo et al., 2013) and displayed the smallest slope in the instability index curve (Fig. 6B). This results are mainly attributed to the stronger repulsive hindrance between liposomal vesicles and higher viscosity caused by the high molecular weight of chitosan (Dammak & Sobral, 2018). As an amphiphilic polyelectrolyte, chitosan combines both electrostatic and viscosifying stabilization mechanisms, which slowed down vesicles movement as encountered under centrifugation (Bouyer, Mekhloufi, Rosilio, Grossiord, & Agnely, 2012). In addition, the viscosity of chitosan increased with its concentration and molecular weight, leading to the slowest vesicles migration to the sedimentation of HCS-H coated Cur-LP. In consideration of the relatively big vesicle size for HCS-coated Cur-LP, we conclude that there is a clear connection between vesicle size and physical stability in chitosan-coated liposomes. Increasing molecular weight and concentration of chitosan could synergistically stabilize curcumin-loaded liposomes. The centrifugal stability results

481 are in good agreement with vesicle size variation results of the storage stability analysis.

482 *3.3 Liposomal membrane properties*

483 The decoration effect of chitosan mainly focused on the enhanced stability of
484 liposomes (section 3.2) in relation to the direct interaction of the coating with liposomal
485 surface. The membranes properties within the liposomes instead have been investigated
486 by two different fluorescence probe methods (section 2.6). Resulting micropolarity and
487 fluidity value of membranes are summarized in Fig. 7. As shown in Fig. 7A, the I_1/I_3
488 values decreased as chitosan concentration increased for Cur-LP. This demonstrates
489 that polar moieties decrease gradually, when more chitosan is deposited on the vesicles,
490 which is acting as a water penetration barrier (Tan et al., 2015). Hence, the highest
491 micropolarity was obtained for Cur-LP due to the absence of a chitosan barrier. That is,
492 in this case pyrene molecules were extensively perturbed by surrounding solvent
493 molecules to form ground state complexes with polar solvents (Heldt et al., 2001). The
494 lower micropolarity of HCS-L compared with LCS-L demonstrates that HCS
495 performed better in caging efficiently vesicles than LCS in case of low chitosan
496 concentration. Further, when the concentration was increased, micropolarity of LCS-
497 coated Cur-LP significantly decreased, while it was not obvious for HCS-coated ones.
498 It is speculated that HCS with longer molecular chains failed to cover the smaller polar
499 moieties on surfaces of liposomes, even when increasing its concentration. Conversely,
500 it might be easier for LCS to shield polar domains due to the smaller molecular volume,
501 which is also reflected in the stronger LCS-concentration dependence in the

micropolarity. Chen found that the permeability of chitosan membranes was inversely proportional to its molecular weight (Chen & Hwa, 1996), which is in line with our results and the interpretation that micropolarity of coated liposomal membranes are more sensitive to chitosan concentration, when LCS coating was used.

The fluorescence polarization of DPH is indicative for membrane fluidity caused by mobility and rotation of phospholipids in liposomal bilayers. All calculated polarizations of chitosan-coated Cur-LP are presented in Fig. 7B. It is observed that as chitosan concentration was increased, the fluidity of liposomal membranes decreased as confirmed in the increased DPH fluorescence polarization, independent of the kind of chitosan used. The results are explained by the hampered lateral movement of phospholipids due to the membrane-inserting hydrophobic moieties of chitosan (Tan, Feng, et al., 2016; Tan et al., 2013). Besides, membrane fluidities in all HCS-coated vesicles being significantly lower than that of LCS-coated ones, illustrates that the longer molecular chains of HCS, the greater the immobilizing of longitudinal motion of phospholipid molecules becomes. Note, that at extreme chitosan concentrations (over 3.0 mg/mL), it is observed that the fluidity of liposomal membranes increased again, which was explained by the onset of membrane disruption on account of the penetration of excessive chitosan into membrane bilayers (Tan et al., 2013). In our study, however, the highest chitosan concentration applied in LCS-H and HCS-H did not exceed 3.125 mg/mL, thus not observing any membrane disturbance. Another reason for the observed membrane disruption by Tan could be attributed to the different

coating method applied, i.e. adding chitosan solution dropwise to liposomal dispersions has the drawback that it might lead to membrane imperfections due to the inhomogeneous chitosan absorption inevitably (Claesson & Ninham, 1992; Henriksen et al., 1994). In contrast, the method of adding liposomes into chitosan solution applied in this study appeared to be more favourable to make excess of chitosan polymer available instantaneously (Henriksen et al., 1994), which effectively decreased the membrane perturbing effects described above.

Based on membranes property studies, the more rigid protective layer formed by chitosan was achieved when increasing the molecular weight and concentration. Hence, the sufficient electrostatic repulsion and compact core-shell structure synergistically improved the stability of Cur-LP against diverse environmental stresses studied above.

3.4 In vitro release study in simulated digestion

Improved physicochemical stability of chitosan-coated Cur-LP obtained above is the premise of sustained release in digestion. Achieving progress in slow release performance for encapsulated curcumin is the final objective of this study. As shown in Fig. 8, since less than 4% of curcumin was released from chitosan-coated liposomes or slightly over 6% from uncoated ones, the simulated mouth phase is not the primary release site for liposomes due to the short duration of this digestion step and the absence of any specific enzyme activity. Most of released curcumin in this phase is attributed to smaller fractions liposomes being surface adsorbed and mechanical disrupted. When liposomes are subjected to gastric digestion, the highest curcumin release rate was

observed in Cur-LP. Over 10% of curcumin was released in the middle of gastric digestion step (75 min). Here, LCS-coated Cur-LP released more curcumin than HCS-coated ones, although the release degree was still not high. It is also well verified that chitosan-coated Cur-LP transport more curcumin into the major digestive site (small intestine). Similar results were obtained in previous studies (Tai et al., 2017; Tan et al., 2014). As expected, the greatest Cur-release took place during the simulated small intestine phase for all liposomes. Cur-LP displayed the fastest release that over 80% of embedded curcumin was released after 250 min digestion. The release rates of LCS-coated liposomes were still higher than HCS-coated ones. Moreover, the release rate of chitosan-coated liposomes was largely dependent with chitosan concentration. Chitosan at higher concentrations slowed the release of curcumin from liposomes, which is consistent with results of improved liposomal stability and reduced membrane fluidity. The liposomal membranes coated by a strong chitosan framework protect curcumin from leakage and degradation by the complex digestive environment, such as digestive movement, human body temperature and various chemicals. The result of *in vitro* simulated digestion reveals that HCS coating with high concentration (about 3 mg/mL) is indeed a promising strategy for further improving the sustained release properties of Cur-LP.

4. Conclusions

In this study, we provide a systematic *in vitro* stability evaluation for Cur-LP coated

by chitosan in terms of different molecular weights and concentrations. Apart from the proved protective effect of chitosan on liposomes in previous studies, this study further reveals that molecular weight and concentration of chitosan play an important role in stabilizing Cur-LP. Both, LCS and HCS coating resulted in better photo and thermal stability, especially for high concentration. As to the storage and centrifugal stability test, increasing chitosan concentration is verified as an effective method in improving stability. The membrane properties studies reveals that the liposomal membranes become more rigid and compact, if molecular weight and concentration of chitosan was increased. The reduced membrane fluidity effectively decreased membrane disruption and leakage of curcumin from the liposomes. This is understood to be the main reason for HCS-H coated liposomes to display the best sustained release property in simulated digestion. The positive effect of chitosan with high molecular weight and concentration on *in vitro* stability is promising for the manufacturing liposomal food with longer shelf-life and strongly improves bioavailability of bioactive compounds as shown for the case of curcumin.

Acknowledgements

This research was financially supported by the National Key R&D Program of China (2016YFD0400804, 2016YFD0400601), the National Natural Science Foundation of China (No. 31371836), the Beijing Natural Science Foundation (No. 6192015). Kedong Tai was financially supported from the China Scholarship Council

586 (CSC) for studying in the United Kingdom.

587

588 **References**

589 Alavi, S., Haeri, A., & Dadashzadeh, S. (2017). Utilization of chitosan-caged liposomes
590 to push the boundaries of therapeutic delivery. *Carbohydrate Polymers, 157*,
591 991-1012.

592 Alehosseini, A., Gomez-Mascaraque, L. G., Martinez-Sanz, M., & Lopez-Rubio, A.
593 (2019). Electrospun curcumin-loaded protein nanofiber mats as active/bioactive
594 coatings for food packaging applications. *Food Hydrocolloids, 87*, 758-771.

595 Anand, P., Kunnumakkara, A. B., Newman, R. A., & Aggarwal, B. B. (2007).
596 Bioavailability of curcumin: Problems and promises. *Molecular Pharmaceutics,*
597 *4*(6), 807-818.

598 Bandak, S., Ramu, A., Barenholz, Y., & Gabizon, A. (1999). Reduced UV-induced
599 degradation of doxorubicin encapsulated in polyethyleneglycol-coated
600 liposomes. *Pharmaceutical Research, 16*(6), 841-846.

601 Bouyer, E., Mekhloufi, G., Rosilio, V., Grossiord, J. L., & Agnely, F. (2012). Proteins,
602 polysaccharides, and their complexes used as stabilizers for emulsions:
603 Alternatives to synthetic surfactants in the pharmaceutical field? *International*
604 *Journal of Pharmaceutics, 436*(1-2), 359-378.

605 Caddeo, C., Manconi, M., Fadda, A. M., Lai, F., Lampis, S., Diez-Sales, O., & Sinico,
606 C. (2013). Nanocarriers for antioxidant resveratrol: Formulation approach,

607 vesicle self-assembly and stability evaluation. *Colloids and Surfaces B-*
608 *Biointerfaces, 111*, 327-332.
609 Chen, R. H., & Hwa, H. D. (1996). Effect of molecular weight of chitosan with the
610 same degree of deacetylation on the thermal, mechanical, and permeability
611 properties of the prepared membrane. *Carbohydrate Polymers, 29*(4), 353-358.
612 Cheng, C., Peng, S. F., Li, Z. L., Zou, L. Q., Liu, W., & Liu, C. M. (2017). Improved
613 bioavailability of curcumin in liposomes prepared using a pH-driven, organic
614 solvent-free, easily scalable process. *Rsc Advances, 7*(42), 25978-25986.
615 Choudhary, V., Shivakumar, H., & Ojha, H. (2019). Curcumin-loaded liposomes for
616 wound healing: Preparation, optimization, in-vivo skin permeation and
617 bioevaluation. *Journal of Drug Delivery Science and Technology, 49*, 683-691.
618 Claesson, P. M., & Ninham, B. W. (1992). Ph-Dependent Interactions between
619 Adsorbed Chitosan Layers. *Langmuir, 8*(5), 1406-1412.
620 Cuomo, F., Cofelice, M., Venditti, F., Ceglie, A., Miguel, M., Lindman, B., & Lopez,
621 F. (2018). In-vitro digestion of curcumin loaded chitosan-coated liposomes.
622 *Colloids and Surfaces B-Biointerfaces, 168*, 29-34.
623 Dammak, I., & Sobral, P. J. A. (2018). Formulation optimization of lecithin-enhanced
624 pickering emulsions stabilized by chitosan nanoparticles for hesperidin
625 encapsulation. *Journal of Food Engineering, 229*, 2-11.
626 Desai, K. G., Liu, C., & Park, H. J. (2006). Characteristics of vitamin C encapsulated
627 tripolyphosphate-chitosan microspheres as affected by chitosan molecular

weight. *Journal of Microencapsulation, 23*(1), 79-90.

Filipovic-Grcic, J., Skalko-Basnet, N., & Jalsenjak, I. (2001). Mucoadhesive chitosan-coated liposomes: characteristics and stability. *Journal of Microencapsulation, 18*(1), 3-12.

Gradauer, K., Barthelmes, J., Vonach, C., Almer, G., Mangge, H., Teubl, B., Roblegg, E., Dunnhaupt, S., Frohlich, E., Bernkop-Schnurch, A., & Prassl, R. (2013). Liposomes coated with thiolated chitosan enhance oral peptide delivery to rats. *Journal of Controlled Release, 172*(3), 872-878.

Grit, M., & Crommelin, D. J. (1993). Chemical stability of liposomes: implications for their physical stability. *Chemistry and physics of lipids, 64*(1-3), 3-18.

Han, H. K., Shin, H. J., & Ha, D. H. (2012). Improved oral bioavailability of alendronate via the mucoadhesive liposomal delivery system. *European Journal of Pharmaceutical Sciences, 46*(5), 500-507.

Hao, J. P., Guo, B., Yu, S. X., Zhang, W. T., Zhang, D. H., Wang, J. L., & Wang, Y. R. (2017). Encapsulation of the flavonoid quercetin with chitosan-coated nano-liposomes. *Lwt-Food Science and Technology, 85*, 37-44.

Hayashi, H., Kono, K., & Takagishi, T. (1998). Temperature-dependent associating property of liposomes modified with a thermosensitive polymer. *Bioconjugate Chemistry, 9*(3), 382-389.

He, H. S., Lu, Y., Qi, J. P., Zhu, Q. G., Chen, Z. J., & Wu, W. (2019). Adapting liposomes for oral drug delivery. *Acta Pharmaceutica Sinica B, 9*(1), 36-48.

649 Heldt, N., Gauger, M., Zhao, J., Slack, G., Pietryka, J., & Li, Y. (2001).
650 Characterization of a polymer-stabilized liposome system. *Reactive &*
651 *Functional Polymers, 48*(1-3), 181-191.
652 Henriksen, I., Smistad, G., & Karlsen, J. (1994). Interactions between Liposomes and
653 Chitosan. *International Journal of Pharmaceutics, 101*(3), 227-236.
654 Henriksen, I., Vagen, S. R., Sande, S. A., Smistad, G., & Karlsen, J. (1997). Interactions
655 between liposomes and chitosan .2. Effect of selected parameters on
656 aggregation and leakage. *International Journal of Pharmaceutics, 146*(2), 193-
657 203.
658 Jeon, S., Yoo, C. Y., & Park, S. N. (2015). Improved stability and skin permeability of
659 sodium hyaluronate-chitosan multilayered liposomes by Layer-by-Layer
660 electrostatic deposition for quercetin delivery. *Colloids and Surfaces B-*
661 *Biointerfaces, 129*, 7-14.
662 Karewicz, A., Bielska, D., Loboda, A., Gzyl-Malcher, B., Bednar, J., Jozkowicz, A.,
663 Dulak, J., & Nowakowska, M. (2013). Curcumin-containing liposomes
664 stabilized by thin layers of chitosan derivatives. *Colloids and Surfaces B-*
665 *Biointerfaces, 109*, 307-316.
666 Kean, T., & Thanou, M. (2010). Biodegradation, biodistribution and toxicity of
667 chitosan. *Advanced Drug Delivery Reviews, 62*(1), 3-11.
668 Laye, C., McClements, D. J., & Weiss, J. (2008). Formation of biopolymer-coated
669 liposomes by electrostatic deposition of chitosan. *Journal of Food Science,*

670 *73*(5), N7-N15.

671 Li, J., Hwang, I. C., Chen, X., & Park, H. J. (2016). Effects of chitosan coating on
672 curcumin loaded nano-emulsion: Study on stability and in vitro digestibility.
673 *Food Hydrocolloids, 60*, 138-147.

674 Li, M. Y., Du, C. Y., Guo, N., Teng, Y. O., Meng, X., Sun, H., Li, S. S., Yu, P., &
675 Galons, H. (2019). Composition design and medical application of liposomes.
676 *European Journal of Medicinal Chemistry, 164*, 640-653.

677 Li, R. W., Deng, L., Cai, Z. W., Zhang, S. Y., Wang, K., Li, L. H., Ding, S., & Zhou,
678 C. R. (2017). Liposomes coated with thiolated chitosan as drug carriers of
679 curcumin. *Materials Science & Engineering C-Materials for Biological*
680 *Applications, 80*, 156-164.

681 Li, Z. Y., Paulson, A. T., & Gill, T. A. (2015). Encapsulation of bioactive salmon
682 protein hydrolysates with chitosan-coated liposomes. *Journal of Functional*
683 *Foods, 19*, 733-743.

684 Liu, W. D., Zhai, Y. J., Heng, X. Y., Che, F. Y., Chen, W. J., Sun, D. Z., & Zhai, G. X.
685 (2016). Oral bioavailability of curcumin: problems and advancements. *Journal*
686 *of Drug Targeting, 24*(8), 694-702.

687 Liu, W. L., Liu, W., Ye, A. Q., Peng, S. F., Wei, F. Q., Liu, C. M., & Han, J. Z. (2016).
688 Environmental stress stability of microencapsules based on liposomes decorated
689 with chitosan and sodium alginate. *Food Chemistry, 196*, 396-404.

690 Liu, Y. J., Liu, D. D., Zhu, L., Gan, Q., & Le, X. Y. (2015). Temperature-dependent

structure stability and in vitro release of chitosan-coated curcumin liposome. *Food Research International, 74*, 97-105.

Ma, P. H., Zeng, Q. H., Tai, K. D., He, X. Y., Yao, Y. Y., Hong, X. F., & Yuan, F. (2017). Preparation of curcumin-loaded emulsion using high pressure homogenization: Impact of oil phase and concentration on physicochemical stability. *Lwt-Food Science and Technology, 84*, 34-46.

Maiti, K., Mukherjee, K., Gantait, A., Saha, B. P., & Mukherjee, P. K. (2007). Curcumin-phospholipid complex: Preparation, therapeutic evaluation and pharmacokinetic study in rats. *International Journal of Pharmaceutics, 330*(1-2), 155-163.

Mujtaba, M., Morsi, R. E., Kerch, G., Elsabee, M. Z., Kaya, M., Labidi, J., & Khawar, K. M. (2019). Current advancements in chitosan-based film production for food technology; A review. *International Journal of Biological Macromolecules, 121*, 889-904.

Nelson, K. M., Dahlin, J. L., Bisson, J., Graham, J., Pauli, G. F., & Walters, M. A. (2017). The Essential Medicinal Chemistry of Curcumin. *Journal of Medicinal Chemistry, 60*(5), 1620-1637.

Park, S. N., Jo, N. R., & Jeon, S. H. (2014). Chitosan-coated liposomes for enhanced skin permeation of resveratrol. *Journal of Industrial and Engineering Chemistry, 20*(4), 1481-1485.

Pavinatto, F. J., Caseli, L., & Oliveira, O. N. (2010). Chitosan in Nanostructured Thin

712 Films. *Biomacromolecules, 11*(8), 1897-1908.
713 Pu, C. F., Tang, W. T., Li, X. D., Li, M., & Sun, Q. J. (2019). Stability enhancement
714 efficiency of surface decoration on curcumin-loaded liposomes: Comparison of
715 guar gum and its cationic counterpart. *Food Hydrocolloids, 87*, 29-37.
716 Shin, G. H., Chung, S. K., Kim, J. T., Joung, H. J., & Park, H. J. (2013). Preparation of
717 Chitosan-Coated Nanoliposomes for Improving the Mucoadhesive Property of
718 Curcumin Using the Ethanol Injection Method. *Journal of Agricultural and*
719 *Food Chemistry, 61*(46), 11119-11126.
720 Tai, K., Rappolt, M., He, X., Wei, Y., Zhu, S., Zhang, J., Mao, L., Gao, Y., & Yuan, F.
721 (2019). Effect of β-sitosterol on the curcumin-loaded liposomes: Vesicle
722 characteristics, physicochemical stability, in vitro release and bioavailability.
723 *Food Chemistry, 293*, 92-102.
724 Tai, K. D., He, X. Y., Yuan, X. D., Meng, K., Gao, Y. X., & Yuan, F. (2017). A
725 comparison of physicochemical and functional properties of icaritin-loaded
726 liposomes based on different surfactants. *Colloids and Surfaces a-*
727 *Physicochemical and Engineering Aspects, 518*, 218-231.
728 Tan, C., Feng, B., Zhang, X. M., Xia, W. S., & Xia, S. Q. (2016). Biopolymer-coated
729 liposomes by electrostatic adsorption of chitosan (chitosomes) as novel delivery
730 systems for carotenoids. *Food Hydrocolloids, 52*, 774-784.
731 Tan, C., Xie, J. H., Zhang, X. M., Cai, J. B., & Xia, S. Q. (2016). Polysaccharide-based
732 nanoparticles by chitosan and gum arabic polyelectrolyte complexation as

carriers for curcumin. *Food Hydrocolloids, 57*, 236-245.

Tan, C., Xue, J., Eric, K., Feng, B., Zhang, X. M., & Xia, S. Q. (2013). Dual Effects of Chitosan Decoration on the Liposomal Membrane Physicochemical Properties As Affected by Chitosan Concentration and Molecular Conformation. *Journal of Agricultural and Food Chemistry, 61*(28), 6901-6910.

Tan, C., Zhang, Y. T., Abbas, S., Feng, B., Zhang, X. M., & Xia, S. Q. (2014). Modulation of the carotenoid bioaccessibility through liposomal encapsulation. *Colloids and Surfaces B-Biointerfaces, 123*, 692-700.

Tan, C., Zhang, Y. T., Abbas, S., Feng, B., Zhang, X. M., Xia, S. Q., & Chang, D. W. (2015). Insights into chitosan multiple functional properties: the role of chitosan conformation in the behavior of liposomal membrane. *Food & Function, 6*(12), 3702-3711.

Tan, H. W., & Misran, M. (2012). Characterization of fatty acid liposome coated with low-molecular-weight chitosan. *Journal of Liposome Research, 22*(4), 329-335.

Tian, M. P., Song, R. X., Wang, T., Sun, M. J., Liu, Y., & Chen, X. G. (2018). Inducing sustained release and improving oral bioavailability of curcumin via chitosan derivatives-coated liposomes. *International Journal of Biological Macromolecules, 120*, 702-710.

Wang, X. Y., & Gao, Y. (2018). Effects of length and unsaturation of the alkyl chain on the hydrophobic binding of curcumin with Tween micelles. *Food Chemistry, 246*, 242-248.

754 Wu, Z. H., Ping, Q. N., Wei, Y., & Lai, J. M. (2004). Hypoglycemic efficacy of
755 chitosan-coated insulin liposomes after oral administration in mice. *Acta*
756 *Pharmacologica Sinica, 25*(7), 966-972.
757 Zheng, B. J., Zhang, Z. P., Chen, F., Luo, X., & McClements, D. J. (2017). Impact of
758 delivery system type on curcumin stability: Comparison of curcumin
759 degradation in aqueous solutions, emulsions, and hydrogel beads. *Food*
760 *Hydrocolloids, 71*, 187-197.
761 Zhou, F., Xu, T., Zhao, Y. J., Song, H. X., Zhang, L. Q., Wu, X. D., & Lu, B. Y. (2018).
762 Chitosan-coated liposomes as delivery systems for improving the stability and
763 oral bioavailability of acteoside. *Food Hydrocolloids, 83*, 17-24.
764

Figure captions & Figures

Fig. 1. Vesicle size distribution of Cur-LP with and without chitosan coating. LCS and HCS represent low and high molecular weight chitosan, respectively; L, M and H represent low, medium and high concentrations of chitosan, respectively. The insert in each size distribution diagram shows the corresponding TEM image of the liposomal dispersion.

Fig. 2. Stability of Cur-LP and different chitosan-decorated Cur-LP in NaCl solution. The relative change rate of vesicle size (%) versus salt concentrations (mM) is presented.

Fig. 3. The photo stability of Cur-LP with and without chitosan coating under UV light irradiance of 0.35 W/m^2 for 6 h.

Fig. 4. The thermal stability of Cur-LP and chitosan-decorated ones in an 80 °C water bath for a period of one hour (10-60 min).

Fig. 5. The relative change rates of vesicle sizes for Cur-LP with and without chitosan coating during storage at 4 °C for three weeks.

Fig. 6. Transmission profiles (A1-A7) and instability index curves (B) of Cur-LP with and without chitosan coating retrieved from LUMisizer measurements at 25 °C. The profiles were recorded every 10 s for 1 h. The abscissa and ordinate in panel A1-A7 represent the test tube position and percentage of light transmission, respectively.

Fig. 7. Membrane characteristics of Cur-LP with and without chitosan coating were investigated by pyrene (A) and DPH (B) at 25 °C, respectively. Each data was expressed as the mean value ± standard deviation (n = 3).

Fig. 8. The kinetic release of curcumin from different formulations during simulated *in vitro* digestion at 37 °C. Values are presented as mean ± standard deviation (n = 3).

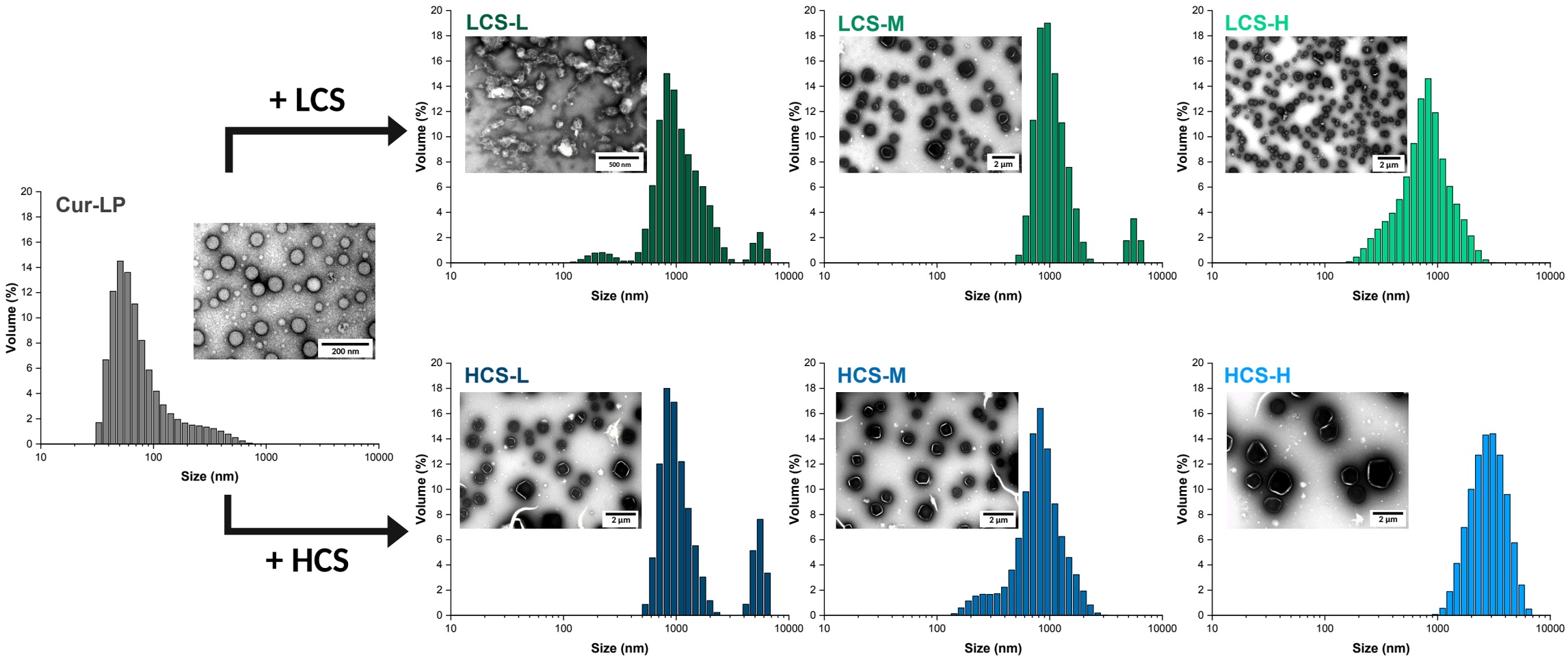
Cur-LP
Volume (%)
Size (nm)
200 nm
+ LCS
+ HCS
LCS-L
LCS-M
LCS-H
HCS-L
HCS-M
HCS-H
500 nm
2 µm

Fig. 1

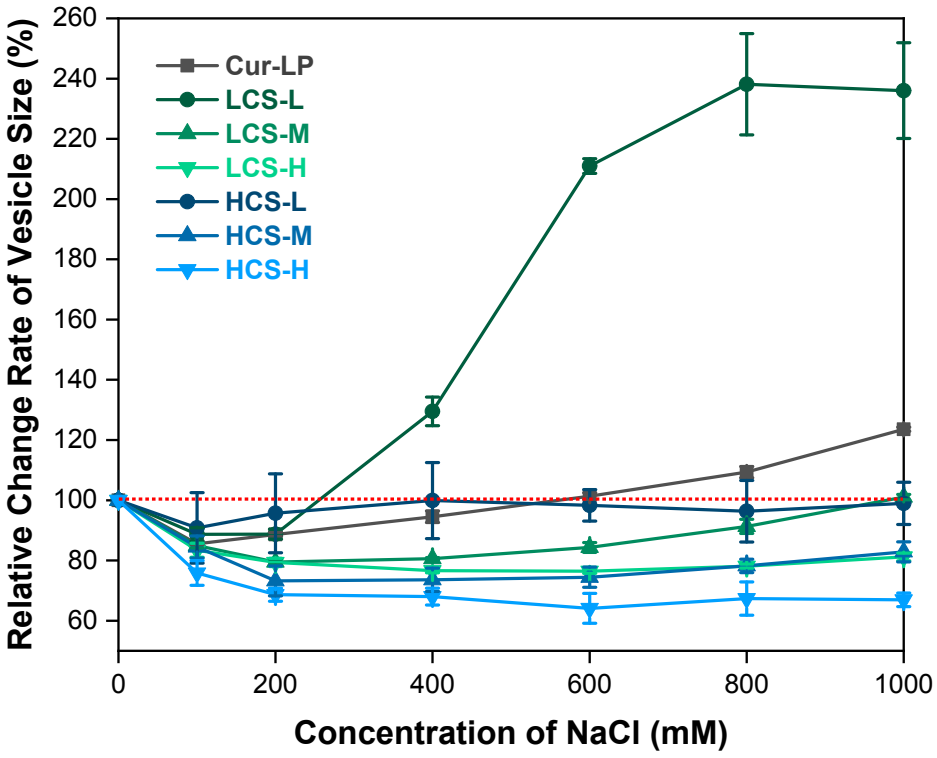
Relative Change Rate of Vesicle Size (%)
260
240
220
200
180
160
140
120
100
80
60
Cur-LP
LCS-L
LCS-M
LCS-H
HCS-L
HCS-M
HCS-H
0
200
400
600
800
1000
Concentration of NaCl (mM)

Fig. 2

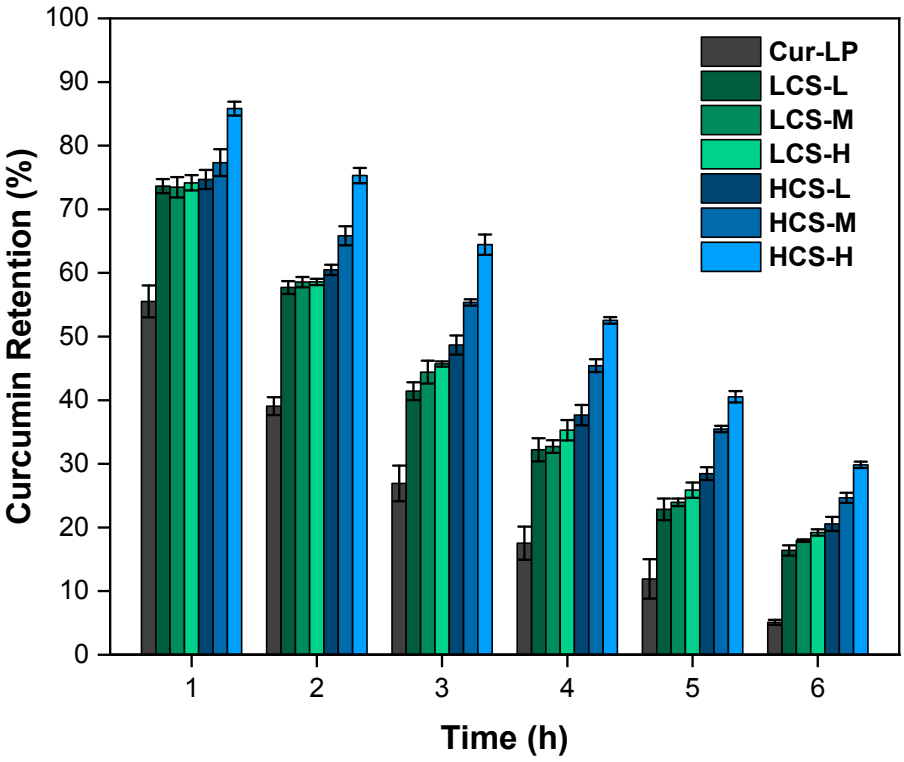
Curcumin Retention (%)
Time (h)
Cur-LP
LCS-L
LCS-M
LCS-H
HCS-L
HCS-M
HCS-H
0
10
20
30
40
50
60
70
80
90
100
1
2
3
4
5
6

Fig. 3

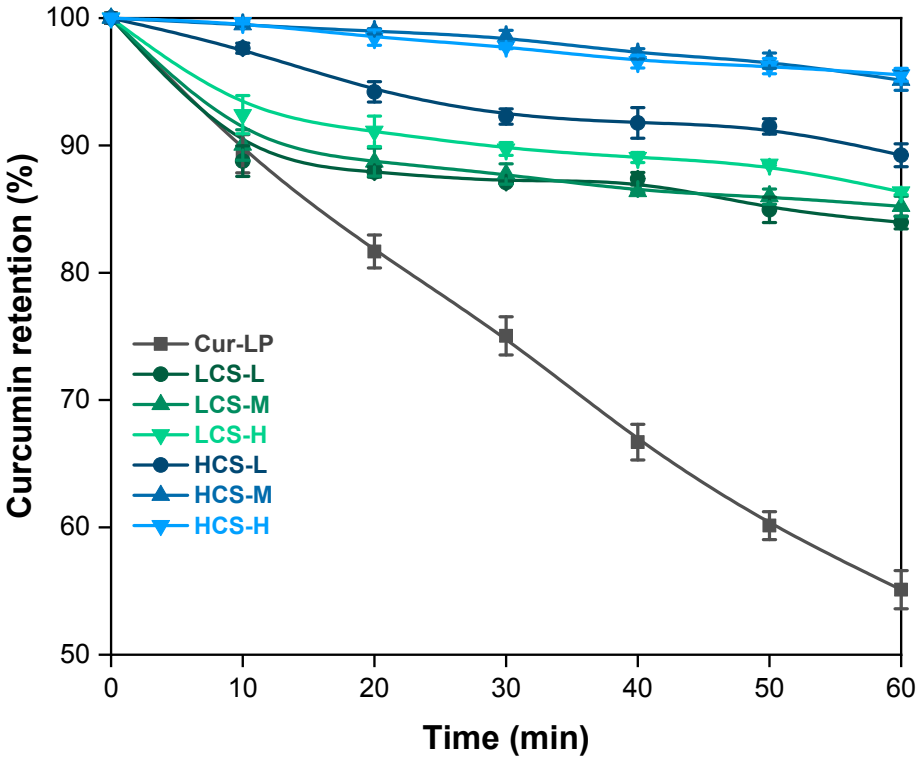
Curcumin retention (%)
Time (min)
100
90
80
70
60
50
0
10
20
30
40
50
60
Cur-LP
LCS-L
LCS-M
LCS-H
HCS-L
HCS-M
HCS-H

Fig. 4

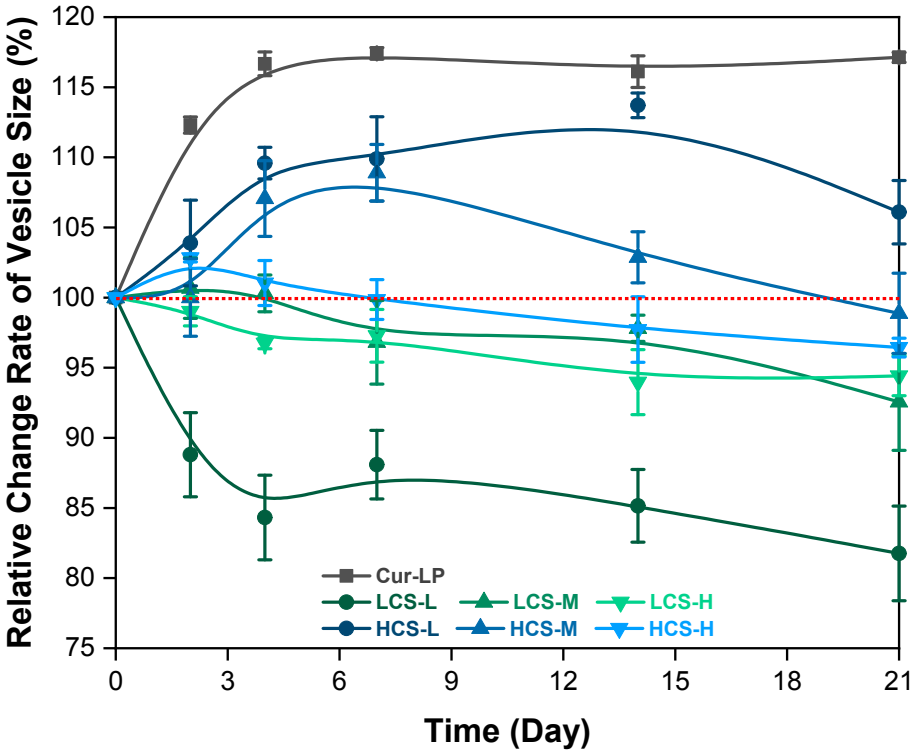
Relative Change Rate of Vesicle Size (%)
120
115
110
105
100
95
90
85
80
75
0
3
6
9
12
15
18
21
Time (Day)
Cur-LP
LCS-L
LCS-M
LCS-H
HCS-L
HCS-M
HCS-H

Fig. 5

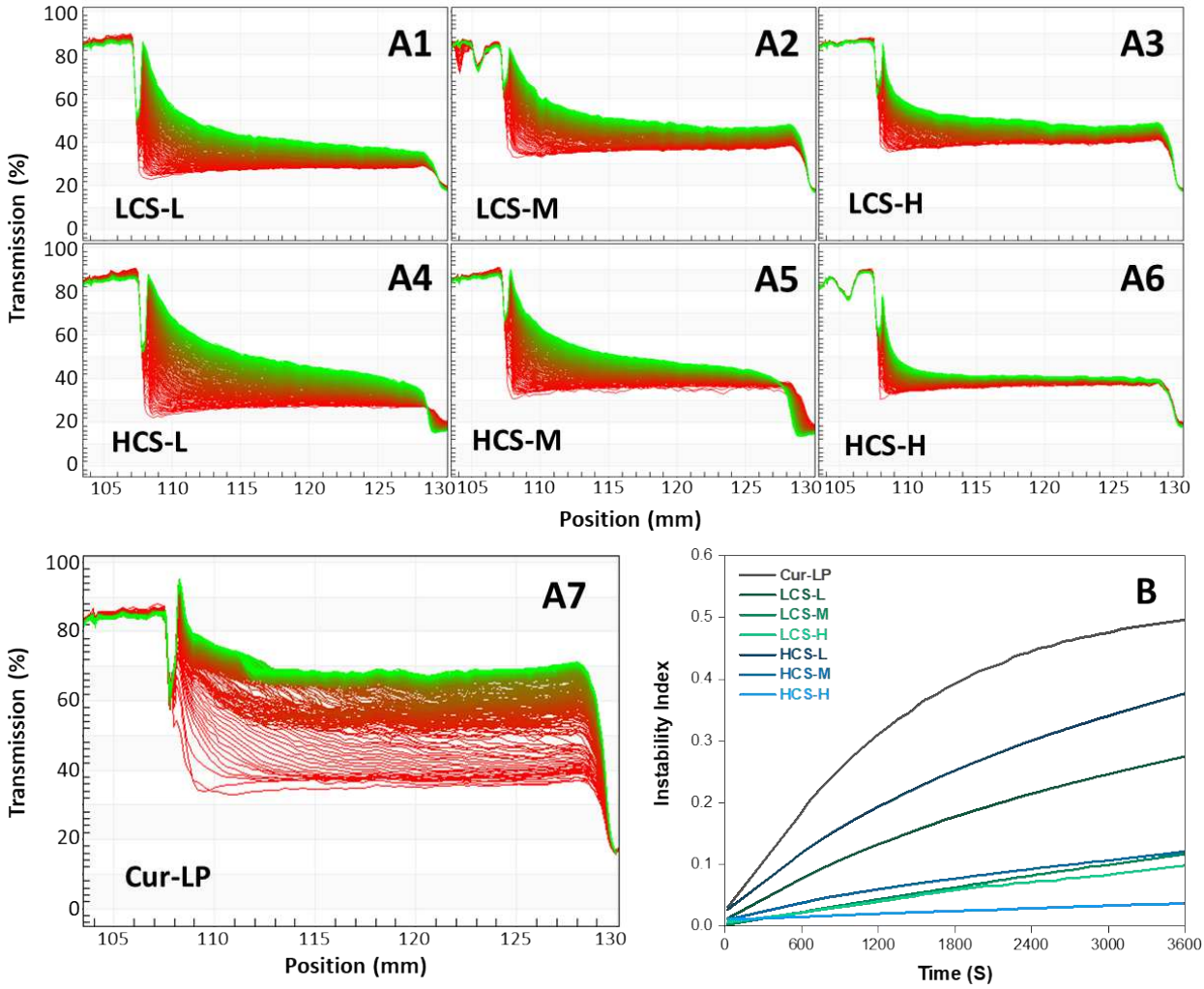
A1
A2
A3
A4
A5
A6
A7
B
LCS-L
LCS-M
LCS-H
HCS-L
HCS-M
HCS-H
Cur-LP
Transmission (%)
Position (mm)
Instability Index
Time (S)

Fig. 6

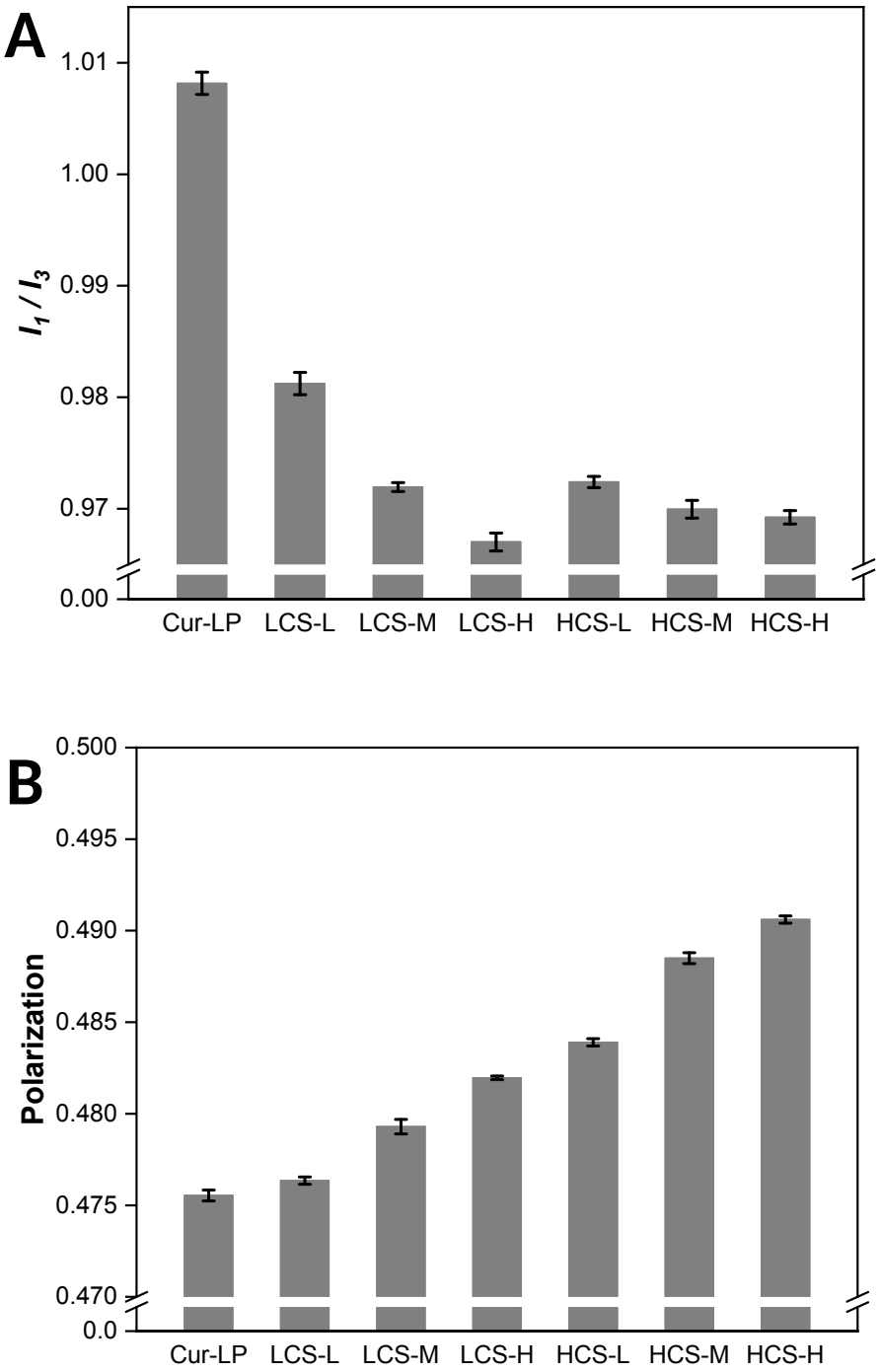
A
1.01
1.00
0.99
0.98
0.97
0.00
I_1 / I_3
Cur-LP
LCS-L
LCS-M
LCS-H
HCS-L
HCS-M
HCS-H
B
0.500
0.495
0.490
0.485
0.480
0.475
0.470
0.0
Polarization
Cur-LP
LCS-L
LCS-M
LCS-H
HCS-L
HCS-M
HCS-H

Fig. 7

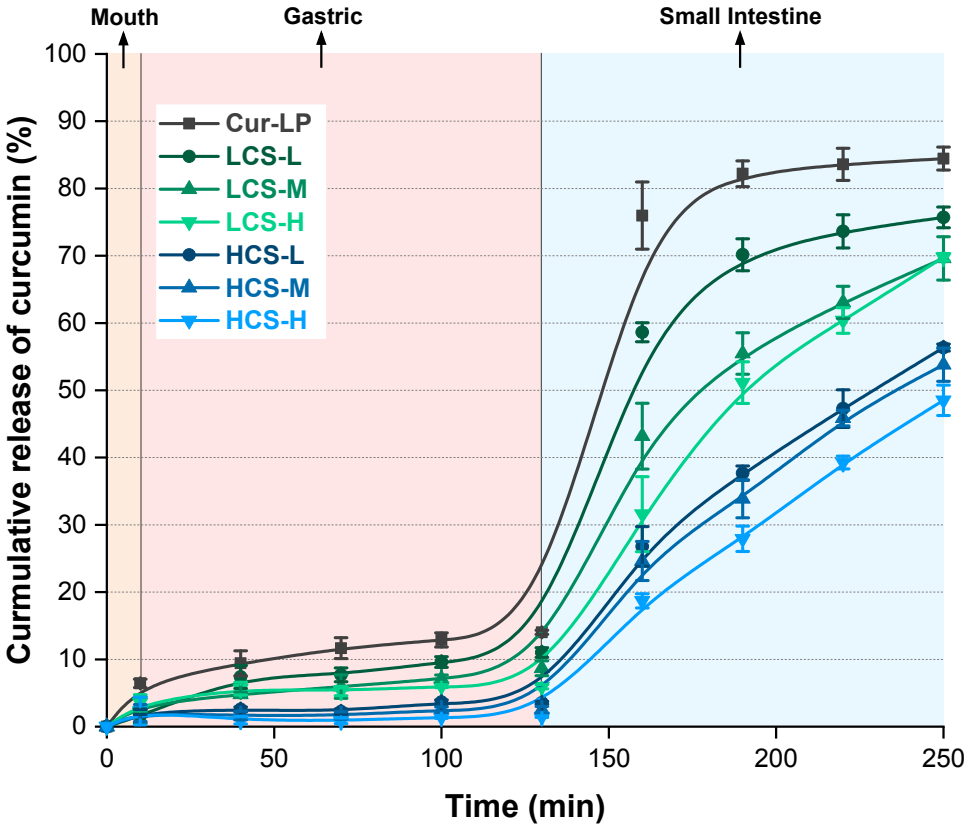
Mouth
Gastric
Small Intestine
Cur-LP
LCS-L
LCS-M
LCS-H
HCS-L
HCS-M
HCS-H
Curmulative release of curcumin (%)
Time (min)
0
10
20
30
40
50
60
70
80
90
100
0
50
100
150
200
250

Fig. 8

TABLE CAPTIONS

Table 1. Size, polydispersity index (PDI), zeta potential and encapsulation efficiency (EE) of curcumin in different formulations.

Liposomes formulations	Vesicle size (nm)	PDI	Zeta potential (mV)	EE (%)
Cur-LP	190 ± 4	0.53 ± 0.01	-45 ± 3	82.41 ± 0.25
LCS-L	1028 ± 30	0.33 ± 0.03	36 ± 2	95.93 ± 0.61
LCS-M	1280 ± 20	0.33 ± 0.01	37 ± 2	96.66 ± 0.70
LCS-H	718 ± 7	0.33 ± 0.03	36 ± 3	94.81 ± 0.30
HCS-L	1324 ± 50	0.35 ± 0.10	36 ± 2	99.19 ± 0.26
HCS-M	1557 ± 40	0.33 ± 0.08	36 ± 2	97.55 ± 0.76
HCS-H	1729 ± 50	0.39 ± 0.11	40 ± 3	95.52 ± 0.66

Conflict of interest

Authors declare that this study does not have any conflict of interest.

Supplementary Data

The stabilization and release performances of curcumin-loaded liposomes coated by high and low molecular weight chitosan

Kedong Tai [a], Michael Rappolt [b], Like Mao [a], Yanxiang Gao [a], Xin Li [c], Fang Yuan [a,*]

[a] Beijing Advanced Innovation Center for Food Nutrition and Human Health, Beijing Laboratory for Food Quality and Safety, Beijing Key Laboratory of Functional Food from Plant Resources, College of Food Science & Nutritional Engineering, China Agricultural University, Beijing 100083, P.R. China

[b] School of Food Science and Nutrition, University of Leeds, Leeds LS2 9JT, U.K.

[c] School of Food Science, Jiangnan University, Wuxi, Jiangsu, 214122, P.R. China

* Corresponding author (Fang Yuan).

Tel: +86-10-62737034

Address: Box 112, No.17 Qinghua East Road, Haidian District, Beijing 100083, China

E-mail: yuanfang0220@cau.edu.cn

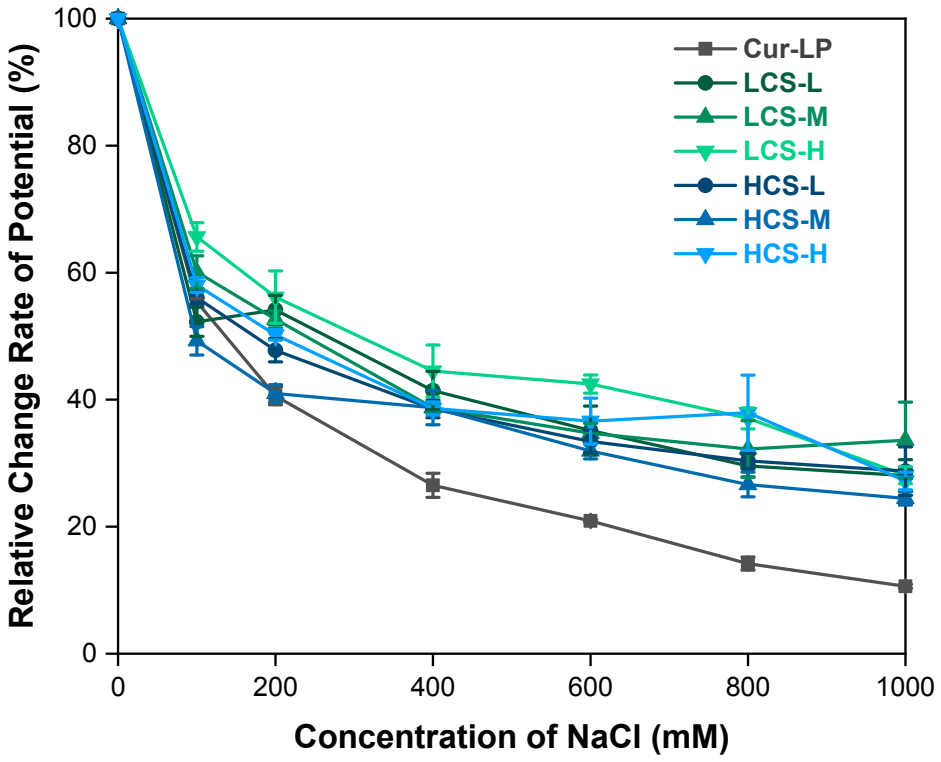

Figure S1. Stability of Cur-LP without and with different chitosan coatings in NaCl solution. The relative change rate of net potential (%) versus salt concentration (mM) is presented. Cur-LP: curcumin-loaded liposomes, LCS and HCS: low and high molecular weight chitosan, L, M and H: low, medium and high concentration of chitosan in final samples.

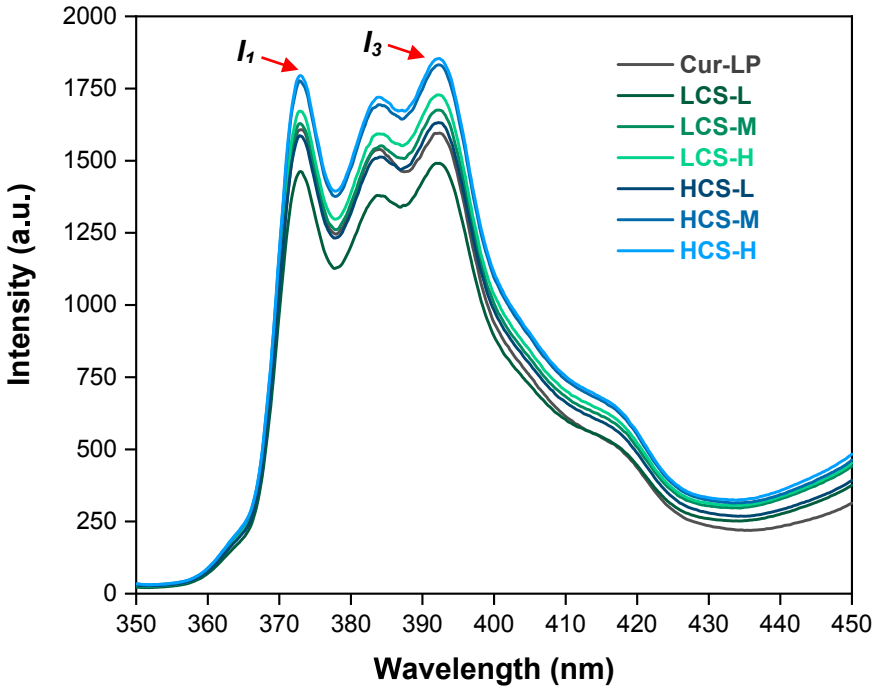

Figure S2. The fluorescence spectra of pyrene in liposomal membranes without and with different chitosan coatings. I_1 and I_3 represent the fluorescence intensity of the first and third peak in the spectra, respectively.